



Contents lists available at ScienceDirect

## International Journal of Solids and Structures

journal homepage: [www.elsevier.com/locate/ijsolstr](http://www.elsevier.com/locate/ijsolstr)

## Degenerate scales for boundary value problems in anisotropic elasticity

Roman Vodička\*, Marek Petřík

Technical University of Košice, Civil Engineering Faculty, Vysokoškolská 4, 042 00 Košice, Slovakia

## ARTICLE INFO

## Article history:

Received 27 June 2014

Received in revised form 25 September 2014

Available online xxxxx

## Keywords:

Degenerate scale

Boundary integral equation

Symmetric Galerkin boundary element method

Generalized plain strain

Anisotropic elasticity

Barnett–Lothe tensor

## ABSTRACT

Degenerate scales usually refer to a size effect which causes non-unique solutions of boundary integral equations for certain type of boundary value problems with a unique solution. They are closely connected to the presence of a logarithmic function in the integral kernel of the single-layer potential operator. The equations of the elasticity theory provide one of the known application fields where degenerate scales appear. The paper discusses conditions and formula for controlling and detection of the degenerate scales in the case of fully anisotropic analysis. No restrictions are considered for the material, only the loading should cause two-dimensional deformation of the anisotropic body. A technique for the evaluation of the degenerate scales is discussed and tested. The examples provide results of special simple cases and demonstrate suitability of the proposed technique in relation to calculation of degenerate scales by numerical solution of pertinent boundary integral equation by the boundary element method.

© 2014 Elsevier Ltd. All rights reserved.

## 1. Introduction

Degenerate scales appear in the solution of some boundary integral equations (BIE). They are provoked in situations affected by the size of the domain, where the BIE has either multiple solutions or does not have a solution at all, while the pertinent boundary value problem (BVP) is uniquely solvable. They arise in the solution of Dirichlet BVP (DBVP) by means of a single-layer potential operator, whose weakly singular integral kernel includes a logarithmic function. The logarithmic character of the kernel is well known in isotropic plane elasticity but it is also retained in the case of anisotropy. In numerical calculations, the degenerate scales may affect the solution of DBVP, if e.g. the boundary element method (BEM) is implemented for pertinent BIE. The above phenomenon represents a well known difficulty appearing in applications of BIEs to the solution of other plane elliptic DBVPs. In potential theory, the degenerate scale for a boundary is characterized by the unit value of the logarithmic capacity of this boundary, see [Jaswon and Symm \(1977\)](#), [McLean \(2000\)](#) and [Yan and Sloan \(1988\)](#). Some approaches for avoiding the non-invertibility of the BIE obtained from the harmonic single-layer potential operator were studied in [Chen et al. \(2014, 2002b\)](#) and [Christiansen \(1982, 1985\)](#). A special attention to the exterior DBVP, especially for the case of domains with several holes, was paid recently in [Chen et al.](#)

(2009b) and [Corfdir and Bonnet \(2013\)](#). Some special cases of boundary contours were discussed in [Chen et al. \(2005, 2009c\)](#) and [Kuo et al. \(2013\)](#). The degenerate scales for the biharmonic single-layer potential were analyzed in depth in [Christiansen \(1998, 2001\)](#) and [Costabel and Dauge \(1996\)](#). Under special conditions, the degenerate scales arise also in solving the Helmholtz equation ([Kress and Spassov, 1983](#)) or the Stokes equation ([Dijkstra and Mattheij, 2008](#)) by BIE.

The degenerate scales in plane isotropic elasticity were determined in numerous analytical and numerical approaches for simple circular, elliptic or annular domains in [Chen et al. \(2002a\)](#), [He et al. \(1996\)](#), [Heise \(1978, 1987\)](#), [Vodička and Mantič \(2008\)](#) and for more general domains in [Kuhn et al. \(1987\)](#) and [Vodička and Mantič \(2004a\)](#). The exterior DBVP was analyzed in [Chen and Lin \(2008\)](#) and [Chen et al. \(2009d\)](#), some examples with asymptotic behavior of degenerate scales was mentioned in [Chen \(2011\)](#) and [Vodička and Mantič \(2004b\)](#) and proved in [Vodička \(2013\)](#). A mathematical proof of the existence of degenerate scales was given in [Constanda \(1994\)](#) and [Vodička and Mantič \(2004b\)](#) and the upper bounds for degenerate scales were proved in [Corfdir and Bonnet \(2014\)](#). Theoretically well based approaches of removing the non-uniqueness from the solution of the single-layer potential BIE were proposed in [Constanda \(1995\)](#) and [Hsiao and Wendland \(1985\)](#).

So far, up to the authors' knowledge, there is no mention about the degenerate scales for anisotropic media in elasticity. Nevertheless, numerous BEM application in this field, e.g. [Blázquez et al. \(2006\)](#), [Mantič and París \(1998\)](#) and [Shiah and Tan \(2000\)](#), may

\* Corresponding author.

E-mail addresses: [roman.vodicka@tuke.sk](mailto:roman.vodicka@tuke.sk) (R. Vodička), [marek.petrik@tuke.sk](mailto:marek.petrik@tuke.sk) (M. Petřík).

under some conditions give rise to this phenomenon. The difference with respect to the standard isotropic analysis is that for a general anisotropic material the inplane and antiplane deformations do not have to be uncoupled so that if for isotropic inplane elasticity there are generally two degenerate scales and for the antiplane elasticity there exists one additional degenerate scale, see e.g. Chen et al. (2009a), there are expected three degenerate scales for general anisotropic elasticity with the displacement field depending on two dimensions, referred also to as generalized plane strain state. The objective of the present paper is, first, to develop a formula calculating the degenerate scales for general anisotropic material with no a priori assumption about material symmetry and, second, to assess its validity by a numerical analysis of the problem implementing the symmetric Galerkin BEM (SGBEM) (Bonnet et al., 1998) for the solution of the pertinent BIE.

In the following part, Section 2, some basic equations are summarized. Simultaneously, basic relations from anisotropic elasticity related to the use of the single-layer potential are mentioned, based on the theory developed in Ting (1996) and Hwu (2010). In the introduction to Section 3, known relations for finding degenerate scales are recalled from Vodička and Mantič (2004b, 2008), the particular relations for anisotropic materials are described in the subsections. Namely, an estimate which guarantees the invertibility of the single-layer potential operator is given in Section 3.1 and derivation of the formula for calculating the degenerate scales is provided in Section 3.2. The formula is tested in the section of examples, Section 4, by an SGBEM code and in one problem also by a comparison with an analytical solution. The paper also includes two appendices which provide a calculation of an integral (Appendix A) required in Section 3.1 and a brief summary of anisotropic fundamental solution (Appendix B) based on the Stroh formalism.

**2. Solution of a Dirichlet boundary value problem by the single-layer potential**

Let us consider an elastic body, a domain  $\Omega \times \langle -h; h \rangle \subset \mathbb{R}^3$ ,  $\Omega \subset \mathbb{R}^2$  with a bounded Lipschitz boundary (McLean, 2000)  $\partial\Omega = \Gamma$  as shown in Fig. 1.

Consider a fixed cartesian coordinate system  $x_i$  ( $i = 1, 2, 3$ ) placed so that  $\Omega$  resides in the coordinate plane  $x_1x_2$ . Let  $\mathbf{u} = (u_1, u_2, u_3)^T$  be the displacement solution of the following Dirichlet problem for the Navier equation in the case of two-dimensional deformations of the body (or the generalized plane strain state) introduced such that no displacement variable depends on the coordinate  $x_3$ :

$$c_{ijkl}u_{k,lj}(x) = 0, \quad x \in \Omega, \tag{1a}$$

$$u_i(x) = g_i(x), \quad x \in \Gamma, \tag{1b}$$

where we denoted  $x = (x_1, x_2)$  and we used the positive definite fourth-order tensor of elastic stiffnesses  $c_{ijkl}$  (Gurtin, 1972) with

no special consideration of material symmetry which is then generally anisotropic. Let us stress that even though the antiplane displacements  $u_3$  are allowed, all deformations depend only on inplane coordinates  $x_1$  and  $x_2$ . It also means that  $l$  and  $j$  could be summed only for 1 and 2, cf. also (4b) below for used elastic parameters.

Let  $\mathbf{U}(x, y) = (U_{ij}(x, y))_{i,j=1,2,3}$  be the symmetric second-order tensor of the fundamental solution of the Navier equation (1a), i.e. displacements at the space point  $x$  due to unit forces

$$\mathbf{F} = (f_1, f_2, f_3) = \left( \begin{pmatrix} 1 \\ 0 \\ 0 \end{pmatrix}, \begin{pmatrix} 0 \\ 1 \\ 0 \end{pmatrix}, \begin{pmatrix} 0 \\ 0 \\ 1 \end{pmatrix} \right) \text{ applied at the point } y = (y_1, y_2).$$

In fact the forces are line forces applied along  $x_3$  axis as long as the loading does not depend on  $x_3$  when the generalized plane strain state is to be considered. The fundamental solution  $\mathbf{U}$  is given according to Ting (1996) as:

$$\begin{aligned} \mathbf{U}(x, y) &= \frac{1}{2\pi} \left[ -\mathbf{H} \ln \frac{r}{r_0} - \pi(\mathbf{H}\mathbf{S}^T(\Theta) + \mathbf{S}\mathbf{H}(\Theta)) + \mathbf{K} \right] \\ &= -\frac{1}{2\pi} \mathbf{H} \ln \frac{r}{r_0} - \mathbf{Z}(\Theta) + \frac{1}{2\pi} \mathbf{K}, \end{aligned} \tag{2}$$

where the polar coordinates  $y_1 = x_1 + r \cos \Theta, y_2 = x_2 + r \sin \Theta$  are used,  $r_0$  is an arbitrary constant to make the argument of logarithm dimensionless (it is usually set to a unit value), and  $\mathbf{K}$  is an arbitrary constant symmetric matrix.

The material characteristics usually defined by the elastic stiffness tensor  $c_{ijkl}$  are included here in the form of the Barnett–Lothe tensors  $\mathbf{H}$  and  $\mathbf{S}$ . All matrices in Eq. (2) can be obtained by known formulae of anisotropic elasticity as follows (see also Ting, 1996):

$$\begin{pmatrix} \mathbf{S}(\Theta) & \mathbf{H}(\Theta) \\ -\mathbf{L}(\Theta) & \mathbf{S}^T(\Theta) \end{pmatrix} = \frac{1}{\pi} \int_0^\Theta \begin{pmatrix} -\mathbf{T}^{-1}(\theta)\mathbf{R}^T(\theta) & \mathbf{T}^{-1}(\theta) \\ -\mathbf{Q}(\theta) + \mathbf{R}(\theta)\mathbf{T}^{-1}(\theta)\mathbf{R}^T(\theta) & -\mathbf{R}(\theta)\mathbf{T}^{-1}(\theta) \end{pmatrix} d\theta, \tag{3a}$$

$$\begin{pmatrix} \mathbf{S} & \mathbf{H} \\ -\mathbf{L} & \mathbf{S}^T \end{pmatrix} = \begin{pmatrix} \mathbf{S}(\pi) & \mathbf{H}(\pi) \\ -\mathbf{L}(\pi) & \mathbf{S}^T(\pi) \end{pmatrix}, \tag{3b}$$

with

$$\begin{pmatrix} \mathbf{Q}(\Theta) & \mathbf{R}(\Theta) \\ \mathbf{R}^T(\Theta) & \mathbf{T}(\Theta) \end{pmatrix} = \begin{pmatrix} \mathbf{I} \cos \Theta & \mathbf{I} \sin \Theta \\ -\mathbf{I} \sin \Theta & \mathbf{I} \cos \Theta \end{pmatrix} \begin{pmatrix} \mathbf{Q} & \mathbf{R} \\ \mathbf{R}^T & \mathbf{T} \end{pmatrix} \begin{pmatrix} \mathbf{I} \cos \Theta & -\mathbf{I} \sin \Theta \\ \mathbf{I} \sin \Theta & \mathbf{I} \cos \Theta \end{pmatrix}. \tag{4a}$$

The relation of the introduced matrices to the elastic stiffnesses  $c_{ijkl}$  is provided by the relations

$$T_{ik} = c_{i2k2}, \quad R_{ik} = c_{i1k2}, \quad Q_{ik} = c_{i1k1}. \tag{4b}$$

Another way of the matrices definition is presented in Appendix B where also some of their useful properties are mentioned.

The solution  $\mathbf{u}$  of DBVP (1) in the indirect method can be expressed in the form of the single-layer potential

$$\mathbf{u}(x) = \int_\Gamma \mathbf{U}(x, y)\varphi(y)d\Gamma(y) = \mathcal{U}\varphi(x), \tag{5}$$

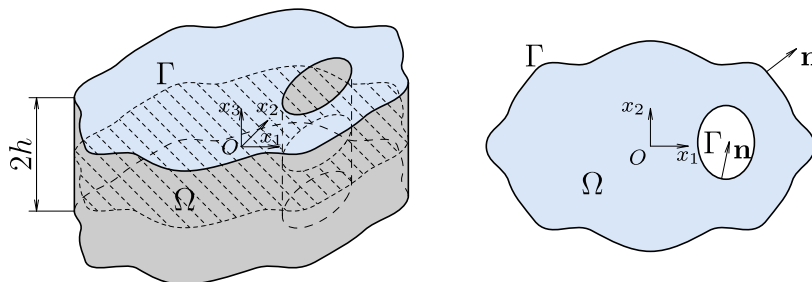


Fig. 1. Description of a cylindrical bounded domain and its cross-section.

where the density  $\boldsymbol{\varphi} = (\varphi_1, \varphi_2, \varphi_3)^\top$  represents a solution of the following BIE:

$$\mathcal{U}_\Gamma \boldsymbol{\varphi} = \mathbf{g}, \tag{6}$$

with the right-hand side containing the boundary conditions (1b). Here, the direct values of the single-layer potential  $\mathcal{U}\boldsymbol{\varphi}(x)$  on the boundary  $\Gamma$ , i.e. for  $x \in \Gamma$ , are distinguished by the subscript  $\Gamma$ . Continuity of the potential  $\mathcal{U}\boldsymbol{\varphi}(x)$  across  $\Gamma$  has been used in obtaining Eq. (6). Note, that displacements  $\mathbf{u} \in [C^\infty(\mathbb{R}^2 \setminus \Gamma)]^3$  in Eq. (5) represent in fact a solution of Navier equation (1a) in  $\mathbb{R}^2 \setminus \Gamma$ .

The same BIE (6) is valid for both interior and exterior DBVPs, where for the exterior DBVPs the function (5) satisfies the consecutive condition at infinity:

$$\mathbf{u}(x) = \mathbf{U}(x, 0)\mathbf{f} + O(\|x\|^{-1})\mathbf{j}, \quad \mathbf{f} = \int_\Gamma \boldsymbol{\varphi}(y)d\Gamma(y), \quad \|x\| \rightarrow \infty, \quad \mathbf{j} = \begin{pmatrix} j_1 \\ j_2 \\ j_3 \end{pmatrix}. \tag{7}$$

### 3. Properties of $\mathcal{U}_\Gamma$ for anisotropic elasticity

Prior to derive a property of guaranteed invertibility and a formula for obtaining the degenerate scales for a generally anisotropic elastic DBVP with deformations dependent on two dimensions (generalized plain strain state), let us recall known formulae independent on the material anisotropy.

The operator  $\mathcal{U}_\Gamma$  is a continuous symmetric linear map between Sobolev spaces (Costabel, 1988; McLean, 2000; Steinbach and Wendland, 2001). In particular, here it is  $\mathcal{U}_\Gamma : [H^{-\frac{1}{2}}(\Gamma)]^3 \mapsto [H^{\frac{1}{2}}(\Gamma)]^3$ . Note that  $[H^{-\frac{1}{2}}(\Gamma)]^3$  is a dual space to  $[H^{\frac{1}{2}}(\Gamma)]^3$  and each time an integral of the form  $\int_\Gamma \tilde{\boldsymbol{\varphi}}^\top \boldsymbol{\varphi} d\Gamma$  appears, it is considered as an expression of duality, extending the inner product in the space of square Lebesgue-integrable functions  $[L_2(\Gamma)]^3$ .

In any case, as follows from the proof in Vodička and Mantič (2004b), the operator  $\mathcal{U}_\Gamma$  is positive in a subset of  $[H^{-\frac{1}{2}}(\Gamma)]^3$  as follows:

$$\text{if } \boldsymbol{\varphi} \in [H^{-\frac{1}{2}}(\Gamma)]^3 : \int_\Gamma \boldsymbol{\varphi} d\Gamma = \mathbf{0} \quad \text{then} \quad \int_\Gamma \boldsymbol{\varphi}^\top [\mathcal{U}_\Gamma \boldsymbol{\varphi}] d\Gamma > 0. \tag{8}$$

Additionally, there was proved in the aforementioned reference that this positivity holds also for a more general subset  $\Omega \subset \mathbb{R}^2$  which is a union of a finite number of domains  $\Omega_m$ ,  $m = 1, \dots, C_\Omega$  and its boundary  $\partial\Omega = \Gamma$  is a union of a finite number of closed Lipschitz curves  $\Gamma_m$ , which do not intersect one another.

Nevertheless, augmenting an operator which is positive in a subset of its domain in the same way as the operator  $\mathcal{U}_\Gamma$  is in (8), leads according to Costabel and Dauge (1996), Vodička and Mantič (2004b) and Hsiao (1986), to an invertible operator. In the present case, the augmented operator converts Eq. (5) to the system

$$\mathcal{U}_\Gamma \boldsymbol{\varphi} - \boldsymbol{\omega} = \mathbf{g}, \quad \int_\Gamma \boldsymbol{\varphi} d\Gamma = \boldsymbol{\xi}, \tag{9}$$

which has for any  $\mathbf{g} \in [H^{\frac{1}{2}}(\Gamma)]^3$  and for each  $\boldsymbol{\xi} \in \mathbb{R}^3$  a unique solution pair  $(\boldsymbol{\varphi}, \boldsymbol{\omega})$ ,  $\boldsymbol{\omega} \in \mathbb{R}^3$ .

Thus, a linear matrix operator  $\mathcal{B}_\Gamma$  with a constant symmetric matrix  $\mathbf{B}_\Gamma \in \mathbb{R}^{3 \times 3}$  (Costabel and Dauge, 1996) can be introduced which for a given  $\boldsymbol{\xi}$  and the fixed  $\mathbf{g} = \mathbf{0}$  finds the corresponding  $\boldsymbol{\omega}$ , i. e.

$$\begin{aligned} \mathbf{B}_\Gamma \boldsymbol{\xi} = \boldsymbol{\omega} \quad &\text{if there exists } \boldsymbol{\varphi} \text{ such that hold both} \\ \mathcal{U}_\Gamma \boldsymbol{\varphi} = \boldsymbol{\omega} \quad &\text{and} \quad \int_\Gamma \boldsymbol{\varphi} d\Gamma = \boldsymbol{\xi}. \end{aligned} \tag{10}$$

The operators  $\mathcal{B}_\Gamma$  and  $\mathcal{U}_\Gamma$  have the same quality of invertibility, symmetry and positiveness, see Costabel and Dauge (1996) and Vodička and Mantič (2004b). Therefore, the task of finding the degenerate scales of the operator  $\mathcal{U}_\Gamma$  can be reduced to the investigation of non-invertibility for the operator  $\mathcal{B}_\Gamma$  which is, in the present case, represented by the square matrix  $\mathbf{B}_\Gamma$  of the dimension three.

#### 3.1. Positiveness of $\mathcal{U}_\Gamma$ for sufficiently small scales

Based on the positiveness of the operator  $\mathcal{U}_\Gamma$  in the subset of  $[H^{-\frac{1}{2}}(\Gamma)]^3$ , Eq. (8), we can state that having the boundary  $\Gamma$  contained in the interior of a circular disk with sufficiently small radius the operator  $\mathcal{U}_\Gamma$  is positive (hence invertible) in  $[H^{-\frac{1}{2}}(\Gamma)]^3$  similarly to Vodička and Mantič (2004b). The task here is to determine the required radius for an arbitrary anisotropic material.

Let  $\Gamma_R$  denote the boundary of the disk with radius  $R$  containing  $\Gamma$ . Then due to (8), we have

$$\int_{\Gamma \cup \Gamma_R} \tilde{\boldsymbol{\varphi}}^\top \mathcal{U}_{\Gamma \cup \Gamma_R} \tilde{\boldsymbol{\varphi}} d\Gamma > 0, \quad \text{if} \quad \int_{\Gamma \cup \Gamma_R} \tilde{\boldsymbol{\varphi}} d\Gamma = \mathbf{0}. \tag{11}$$

for all appropriate non-zero  $\tilde{\boldsymbol{\varphi}} \in [H^{-\frac{1}{2}}(\Gamma \cup \Gamma_R)]^3$ .

Let us take  $\tilde{\boldsymbol{\varphi}}$  in the form

$$\tilde{\boldsymbol{\varphi}}(x) = \begin{cases} \boldsymbol{\varphi}(x) & x \in \Gamma \\ \boldsymbol{\omega} & x \in \Gamma_R \end{cases}, \tag{12}$$

with  $\boldsymbol{\omega}$  chosen so that the condition in (11) is satisfied. Let  $\mathbf{c} = \int_\Gamma \boldsymbol{\varphi} d\Gamma$ , then

$$0 = \int_{\Gamma \cup \Gamma_R} \tilde{\boldsymbol{\varphi}} d\Gamma = \int_\Gamma \boldsymbol{\varphi} d\Gamma + \int_{\Gamma_R} \boldsymbol{\omega} d\Gamma = \mathbf{c} + 2\pi R \boldsymbol{\omega}. \tag{13}$$

Decomposing the integral in (11) yields

$$\begin{aligned} 0 < \int_\Gamma \boldsymbol{\varphi}^\top \mathcal{U}_\Gamma \boldsymbol{\varphi} d\Gamma + \int_\Gamma \boldsymbol{\varphi}^\top(x) \left[ \int_{\Gamma_R} \mathbf{U}(x, y) \boldsymbol{\omega} d\Gamma(y) \right] d\Gamma(x) \\ + \int_{\Gamma_R} \boldsymbol{\omega}^\top \left[ \int_\Gamma \mathbf{U}(x, y) \boldsymbol{\varphi}(y) d\Gamma(y) \right] d\Gamma(x) + \boldsymbol{\omega}^\top \left[ \int_{\Gamma_R} \mathbf{U}(x, y) d\Gamma(y) \right] \boldsymbol{\omega}, \end{aligned} \tag{14}$$

where the second and the third integrals are equal to each other due to the symmetry of the integral kernel of  $\mathcal{U}$ . The integral of  $\mathbf{U}$  along a circle is calculated in Appendix A, cf. Eq. (41)

$$\int_{\Gamma_R} \mathbf{U}(x, y) d\Gamma(y) = -R \left( \ln \frac{R}{r_0} \mathbf{H} + \bar{\mathbf{Z}} - \boldsymbol{\kappa} \right), \tag{15}$$

where  $\bar{\mathbf{Z}} = 2 \int_0^\pi \mathbf{Z}(\Theta) d\Theta$ .

If simultaneously with (15), the relation (13) is substituted into (14), the second integral becomes

$$\mathbf{c}^\top \left[ -R \left( \ln \frac{R}{r_0} \mathbf{H} + \bar{\mathbf{Z}} - \boldsymbol{\kappa} \right) \right] \boldsymbol{\omega} = \frac{1}{2\pi} \mathbf{c}^\top \left( \ln \frac{R}{r_0} \mathbf{H} + \bar{\mathbf{Z}} - \boldsymbol{\kappa} \right) \mathbf{c}, \tag{16a}$$

and the fourth integral renders

$$2\pi R \boldsymbol{\omega}^\top \left[ -R \left( \ln \frac{R}{r_0} \mathbf{H} + \bar{\mathbf{Z}} - \boldsymbol{\kappa} \right) \right] \boldsymbol{\omega} = -\frac{1}{2\pi} \mathbf{c}^\top \left[ \left( \ln \frac{R}{r_0} \mathbf{H} + \bar{\mathbf{Z}} - \boldsymbol{\kappa} \right) \right] \mathbf{c}. \tag{16b}$$

Recall that  $\mathbf{H}$  is symmetric positive definite, see Ting (1996), hence there exists a symmetric positive definite matrix  $\mathbf{H}^{\frac{1}{2}}$  such that  $\mathbf{H}^{\frac{1}{2}} \mathbf{H}^{\frac{1}{2}} = \mathbf{H}$  and also its inverse  $\mathbf{H}^{-\frac{1}{2}}$ . Hence, we see that Eq. (14) converts to the inequality

$$\begin{aligned} \int_\Gamma \boldsymbol{\varphi}^\top \mathbf{U}_\Gamma \boldsymbol{\varphi} d\Gamma > -\frac{1}{2\pi} \mathbf{c}^\top \left( \ln \frac{R}{r_0} \mathbf{H} + \bar{\mathbf{Z}} - \boldsymbol{\kappa} \right) \mathbf{c} \\ = \frac{1}{2\pi} \mathbf{c}^\top \mathbf{H}^{\frac{1}{2}} \left( \ln \frac{r_0}{R} \mathbf{I} - \mathbf{H}^{-\frac{1}{2}} (\bar{\mathbf{Z}} - \boldsymbol{\kappa}) \mathbf{H}^{-\frac{1}{2}} \right) \mathbf{H}^{\frac{1}{2}} \mathbf{c}. \end{aligned} \tag{17}$$

The last term includes, for sufficiently small  $R$ , a symmetric positive definite matrix  $\ln \frac{r_0}{R} \mathbf{I} - \mathbf{H}^{-\frac{1}{2}}(\bar{\mathbf{Z}} - \mathbf{K})\mathbf{H}^{-\frac{1}{2}}$ , therefore the integral in Eq. (17) must be then positive for any non-zero  $\boldsymbol{\varphi}$ . The bound can be found e.g. upon knowing the greatest eigenvalue  $\sigma_{\max}$  of the symmetric matrix  $\mathbf{H}^{-\frac{1}{2}}(\bar{\mathbf{Z}} - \mathbf{K})\mathbf{H}^{-\frac{1}{2}}$  (may be also negative) which gives the sufficient  $R$  from the condition  $\ln \frac{r_0}{R} > \sigma_{\max}$ , i.e.  $R < e^{-\sigma_{\max} r_0}$ . This estimate provides also a guaranty for Eq. (6) to have a unique solution, if a suitable length unit is chosen resulting in sufficiently small dimensions of  $\Gamma$ .

It should also be stressed the dependence of the estimate for  $R$  on the constant  $r_0$  which can then eliminate occurrence of the degenerate scales in practical calculations. In a special case with  $r_0 = 1$  and  $\mathbf{K} = \bar{\mathbf{Z}}$ , the relation (17) renders pretty simple estimation, because the right-hand side reduces to  $\frac{1}{2\pi} \mathbf{c}^\top (\ln \frac{1}{R} \mathbf{H}) \mathbf{c}$  and the condition of guaranteed positivity is  $R < 1$ .

3.2. Scaling and degenerate scales

The degenerate scales appear for any shape of a domain and reflect only a magnifying factor for a set of differently scaled domains. Then, the occurrence of degenerate scales is related to the way how the operator  $\mathcal{U}_\Gamma$  modifies upon scaling the domain. First, let us observe, how the change of domain scale changes the operator. The reasoning is similar to that used in Vodička and Mantič (2004b).

Let us denote the scaling factor  $\rho > 0$  and introduce the scaled boundary  $\rho\Gamma$  by the definition  $\rho\Gamma = \{\rho\mathbf{x} \in \mathbb{R}^2 \mid \mathbf{x} \in \Gamma\}$ . For each  $\rho$  a dilation operator  $\mathcal{M}_\rho$  can be introduced. It is defined on an appropriate function space over  $\Gamma$ :

$$(\mathcal{M}_\rho \boldsymbol{\varphi})(\tilde{\mathbf{y}}) = \boldsymbol{\varphi}\left(\frac{\tilde{\mathbf{y}}}{\rho}\right) = \tilde{\boldsymbol{\varphi}}(\tilde{\mathbf{y}}), \quad \text{for } \tilde{\mathbf{y}} \in \rho\Gamma. \tag{18}$$

Now we can apply the operator  $\mathcal{U}_{\rho\Gamma}$  to a function  $\tilde{\boldsymbol{\varphi}} \in [H^{-\frac{1}{2}}(\rho\Gamma)]^3$

$$\begin{aligned} \mathcal{U}_{\rho\Gamma} \tilde{\boldsymbol{\varphi}}(\rho\mathbf{x}) &= \mathcal{U}_{\rho\Gamma} \mathcal{M}_\rho \boldsymbol{\varphi}(\rho\mathbf{x}) = \int_{\rho\Gamma} \mathbf{U}(\rho\mathbf{x}, \tilde{\mathbf{y}}) \mathcal{M}_\rho \boldsymbol{\varphi}(\tilde{\mathbf{y}}) d(\rho\Gamma)(\tilde{\mathbf{y}}) \\ &= \int_\Gamma \mathbf{U}(\rho\mathbf{x}, \rho\mathbf{y}) \boldsymbol{\varphi}(\mathbf{y}) \rho d\Gamma(\mathbf{y}) \\ &= \rho \int_\Gamma \left[ -\frac{1}{2\pi} \mathbf{H} \ln \frac{\rho \|\mathbf{y} - \mathbf{x}\|}{r_0} - \mathbf{Z}(\Theta) + \frac{1}{2\pi} \mathbf{K} \right] \boldsymbol{\varphi}(\mathbf{y}) d\Gamma(\mathbf{y}) \\ &= \rho \left[ \int_\Gamma \mathbf{U}(\mathbf{x}, \mathbf{y}) \boldsymbol{\varphi}(\mathbf{y}) d\Gamma(\mathbf{y}) - \frac{1}{2\pi} \mathbf{H} \ln \rho \int_\Gamma \boldsymbol{\varphi}(\mathbf{y}) d\Gamma(\mathbf{y}) \right] \\ &= \rho \left[ \mathcal{U}_\Gamma \boldsymbol{\varphi}(\mathbf{x}) - \frac{1}{2\pi} \mathbf{H} \ln \rho \int_\Gamma \boldsymbol{\varphi} d\Gamma \right]. \end{aligned} \tag{19}$$

Realize that if  $\xi = \int_\Gamma \boldsymbol{\varphi} d\Gamma$ , calculating the integral of  $\tilde{\boldsymbol{\varphi}} = \mathcal{M}_\rho \boldsymbol{\varphi}$  provides  $\xi_\rho$  as

$$\xi_\rho = \int_{\rho\Gamma} \tilde{\boldsymbol{\varphi}}(\tilde{\mathbf{x}}) d(\rho\Gamma) = \rho \int_\Gamma \boldsymbol{\varphi}(\mathbf{x}) d\Gamma = \rho \xi. \tag{20}$$

Thus, we can rewrite (19) in the form

$$\mathcal{U}_{\rho\Gamma} \mathcal{M}_\rho \boldsymbol{\varphi}(\tilde{\mathbf{x}}) = \rho (\mathcal{M}_\rho \mathcal{U}_\Gamma \boldsymbol{\varphi})(\tilde{\mathbf{x}}) - \frac{1}{2\pi} \ln \rho \mathbf{H} \xi_\rho. \tag{21}$$

If  $\boldsymbol{\varphi}$  is considered as the solution of Eq. (6) with a constant right-hand side, written due to Eq. (10) as  $\mathcal{U}_\Gamma \boldsymbol{\varphi} = \mathbf{B}_\Gamma \xi$ , it provides the relations valid for the scaled boundary  $\rho\Gamma$

$$\begin{aligned} \mathbf{B}_{\rho\Gamma} \xi_\rho &= \mathcal{U}_{\rho\Gamma} \mathcal{M}_\rho \boldsymbol{\varphi} = \rho \mathcal{M}_\rho \mathbf{B}_\Gamma \xi - \frac{1}{2\pi} \ln \rho \mathbf{H} \xi_\rho \\ &= \mathbf{B}_\Gamma \xi_\rho - \frac{1}{2\pi} \ln \rho \mathbf{H} \xi_\rho, \end{aligned} \tag{22}$$

which renders the transformation relation for  $\mathbf{B}_\Gamma$  upon scaling. As Eq. (22) is valid for any  $\xi_\rho$ , the matrix  $\mathbf{B}_\Gamma$  obeys the equation

$$\mathbf{B}_{\rho\Gamma} = \mathbf{B}_\Gamma - \frac{1}{2\pi} \ln \rho \mathbf{H}. \tag{23}$$

Having in mind that  $\rho_c$  is the degenerate scale factor if and only if the matrix  $\mathbf{B}_{\rho_c\Gamma}$  is singular, leads to solving the equation

$$\det \left( \mathbf{B}_\Gamma - \frac{1}{2\pi} \ln \rho_c \mathbf{H} \right) = 0, \tag{24}$$

which contains two known matrices:  $\mathbf{B}_\Gamma$  from Eq. (10) depending on the shape and size of  $\Gamma$  and  $\mathbf{H}$  from Eq. (3b) containing material parameters. Let  $\sigma$  denote an eigenvalue of the symmetric matrix  $\mathbf{H}^{-\frac{1}{2}} \mathbf{B}_\Gamma \mathbf{H}^{-\frac{1}{2}}$ , then  $\sigma = \frac{1}{2\pi} \ln \rho_c$  and the formula for the degenerate scale factors becomes

$$\rho_c = e^{2\pi\sigma}. \tag{25}$$

There exist three real eigenvalues  $\sigma_i, i = 1, 2, 3$ , not necessarily different, and pertinent orthogonal eigenvectors  $\boldsymbol{\eta}_i$  of the symmetric matrix  $\mathbf{H}^{-\frac{1}{2}} \mathbf{B}_\Gamma \mathbf{H}^{-\frac{1}{2}}$ . On obtaining the degenerate scale factors from (22), the vector  $\xi_\rho$  should be one of the following vectors  $\xi_i = \mathbf{H}^{-\frac{1}{2}} \boldsymbol{\eta}_i$ . These vectors, however, are not necessarily orthogonal for a general anisotropic material with arbitrary orientation of the material axes unless  $\mathbf{H}$  is diagonal. The vectors  $\xi_i$  determine the integral of  $\boldsymbol{\varphi}$  on degenerate scale. If  $\boldsymbol{\varphi}$  expresses tractions, the vector  $\xi_i$  defines the orientation of the total force which solves Eq. (6) on an exterior domain to  $\Gamma$  with the zero right-hand side and the condition at infinity (7).

It should be noted that instead of the symmetric matrix  $\mathbf{H}^{-\frac{1}{2}} \mathbf{B}_\Gamma \mathbf{H}^{-\frac{1}{2}}$ , possibly nonsymmetric matrices  $\mathbf{H}^{-1} \mathbf{B}_\Gamma$  or  $\mathbf{B}_\Gamma \mathbf{H}^{-1}$  can be used to find the degenerate scales. Accordingly, the relation between  $\boldsymbol{\eta}_i$  and  $\xi_i$  changes.

4. Examples

A couple of examples have been chosen to cover simple domain shapes. The geometries considered are: an elliptic region and a rectangular region. Our attention is focused on calculation of degenerate scale factors  $\rho_c$  for both geometrical forms. In all present numerical calculations, the single-layer boundary integral operator  $\mathcal{U}_\Gamma$  with the constants  $r_0 = 1$  and  $\mathbf{K} = \mathbf{0}$  in the operator kernel (2) has been used. Evaluation of degenerate scales is initiated by a numerical solution of the system (9) with  $\mathbf{g} = \mathbf{0}$  for three linearly independent choices of  $\boldsymbol{\omega}$ :  $\boldsymbol{\omega}_1 = (1, 0, 0)^\top$ ,  $\boldsymbol{\omega}_2 = (0, 1, 0)^\top$ , and  $\boldsymbol{\omega}_3 = (0, 0, 1)^\top$ . The solutions enable to find an approximation of the matrix  $\mathbf{B}_\Gamma$  for a particular non-degenerate scale. Denoting the pertinent  $\xi$  by  $\xi_1, \xi_2$ , and  $\xi_3$ , respectively, the matrix  $\mathbf{B}_\Gamma$  can be obtained as  $\mathbf{B}_\Gamma = (\xi_1, \xi_2, \xi_3)^{-1}$ . If necessary, it is possible to scale the domain such that the degenerate scale phenomenon is not in effect, e. g. to fit the domain into a disk of required radius according to Eq. (17) the text below. Finally, using Eqs. (23) and (25), the degenerate scale factors  $\rho_c$  are calculated solving a generalized eigenvalue problem for the matrix  $\mathbf{B}_\Gamma$ .

An SGBEM code with continuous linear elements (Ivančo and Vodička, 2012), has been used to solve numerically the BIE in (9). The used BEM meshes were either uniform, along all straight and circular parts of boundaries, or naturally quasi-uniform, along elliptic boundaries. The element number is kept constant in each particular example when the domain is scaled.

As long as the degenerate scales are the same for interior and exterior BVPs, the first example was also solved analytically as a problem of a rigid elliptic inclusion in an infinite plane. The form of the analytical solution for this problem was taken from Ting (1996) and serves for justification of the formula used in numerical analysis.

The material parameters are chosen to obtain various anisotropic materials. They include an example of a cubic material (crystallized aluminum (Simmons and Wang, 1971), denoted C), an orthotropic

**Table 1**  
Elastic constants  $c_{ijkl}$  of the materials, ( $\times 10^3$  MPa).

$ijkl$	1111	1122	1133	1113	2222	2233	2213	3333	3313	2323	2312	1313	1212
O	14.4	0.89	0.49	0	1.2	0.48	0	0.47	0	0.05	0	0.47	0.57
C	107.3	60.9	MS	0	MS	MS	0	MS	0	28.3	0	MS	MS
M	21.2	1.6	11.5	-0.47	27.9	0.6	-7.4	34.0	0.5	10.8	3.3	11.2	10.0

material (wood (Požgaj et al., 1997), denoted O) and a monoclinic material (a potassium cobaltcyanide crystal (Chou, 1970), denoted M) with a plane of symmetry perpendicular to the axis  $x_2$ . Their elastic stiffnesses picked up from the aforementioned references are summarized in Table 1. The other components of the elastic tensor  $c_{ijkl}$  are either zero or equal to one of the values in the table due to the tensor symmetry. The items ‘MS’ are equal to one of the other given parameters according to the cubic material symmetries.

The material parameters can be substituted into Eq. (4b) to obtain pertinent material matrices: for the material O

$$\begin{aligned} \mathbf{T}_O &= \begin{pmatrix} 0.57 & 0 & 0 \\ 0 & 1.2 & 0 \\ 0 & 0 & 0.05 \end{pmatrix}, & \mathbf{R}_O &= \begin{pmatrix} 0 & 0.89 & 0 \\ 0.57 & 0 & 0 \\ 0 & 0 & 0 \end{pmatrix}, \\ \mathbf{Q}_O &= \begin{pmatrix} 14.4 & 0 & 0 \\ 0 & 0.57 & 0 \\ 0 & 0 & 0.47 \end{pmatrix}, \end{aligned} \quad (26a)$$

for the material C

$$\begin{aligned} \mathbf{T}_C &= \begin{pmatrix} 28.3 & 0 & 0 \\ 0 & 107.3 & 0 \\ 0 & 0 & 28.3 \end{pmatrix}, & \mathbf{R}_C &= \begin{pmatrix} 0 & 60.9 & 0 \\ 28.3 & 0 & 0 \\ 0 & 0 & 0 \end{pmatrix}, \\ \mathbf{Q}_C &= \begin{pmatrix} 107.3 & 0 & 0 \\ 0 & 28.3 & 0 \\ 0 & 0 & 28.3 \end{pmatrix}, \end{aligned} \quad (26b)$$

and for the material M

$$\begin{aligned} \mathbf{T}_M &= \begin{pmatrix} 10.0 & 0 & 3.3 \\ 0 & 27.9 & 0 \\ 3.3 & 0 & 10.8 \end{pmatrix}, & \mathbf{R}_M &= \begin{pmatrix} 0 & 1.6 & 0 \\ 10.0 & 0 & 3.3 \\ 0 & -7.4 & 0 \end{pmatrix}, \\ \mathbf{Q}_M &= \begin{pmatrix} 21.2 & 0 & -0.47 \\ 0 & 10.0 & 0 \\ -0.47 & 0 & 11.2 \end{pmatrix}. \end{aligned} \quad (26c)$$

They also provide the expressions for the other material dependent matrices in Eqs. (3) and (4).

Material symmetries affect the structure of the matrices  $\mathbf{T}$ ,  $\mathbf{R}$  and  $\mathbf{Q}$  which can result to uncoupling of antiplane and inplane deformations. If the material has a sufficient number of symmetry planes and the symmetry planes coincide with the defined coordinate system, as occurs for materials O and C, the first two rows and columns of the matrices are not coupled with the third ones, e.g. in  $\mathbf{T}_C$  we have  $T_{C13} = T_{C23} = T_{C31} = T_{C32} = 0$ . This uncoupling then also transfers to the solution of pertinent BVP (inplane deformations ( $u_1, u_2$ ) and antiplane deformations  $u_3$ ) and to the degenerate scales as well (two degenerate scales for a BVP with the inplane deformations and one for a BVP with the antiplane deformations). Nevertheless, the material M provides only one symmetry plane which is not sufficient to uncouple the antiplane and inplane deformations as e.g.  $T_{M13} \neq 0$ . It results to coupling of the degenerate scales for inplane and antiplane deformations as well.

To follow the general anisotropic case, all three degenerate scales will be searched for in all solved examples.

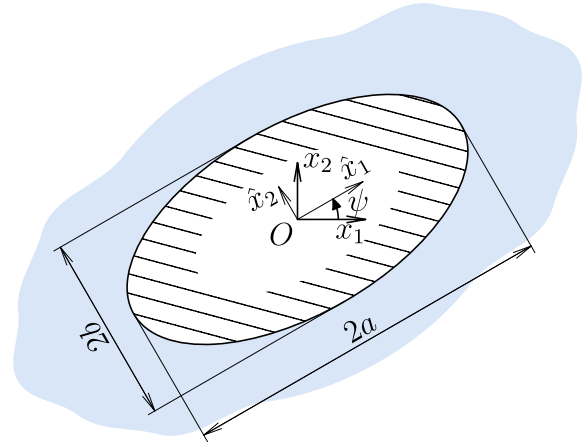


Fig. 2. A rigid elliptic inclusion.

#### 4.1. An ellipse

First, let us consider an elliptic domain as shown in Fig. 2. In this particular case, we can compare the numerical results with analytical ones even for a rotated ellipse, derived from the relations obtained from Ting (1996).

##### 4.1.1. Analytical solution

We start with the analytical solution. Unlike the theory developed for the real-form fundamental solution, here the Stroh formalism with complex-form fundamental solution is used. Necessary relations are gather in Appendix B. The fundamental solution (2) is now given by the relation (42). A degenerate scale pertains to such a scaled domain for which the solution of the exterior BVP with zero prescribed displacements on the boundary, see Fig. 2, provides a non-vanishing solution obeying the relation (7). Thus, the degenerate scales can be found, if the solution for the elliptic rigid inclusion given in Ting (1996) as

$$\mathbf{u}(\mathbf{x}) = \frac{1}{\pi} \Im(\mathbf{A} \text{diag}(\ln \zeta_1, \ln \zeta_2, \ln \zeta_3) \mathbf{A}^T) \mathbf{f} = \frac{1}{\pi} \Im(\mathbf{A}(\ln \zeta_*) \mathbf{A}^T) \mathbf{f}, \quad (27a)$$

with

$$\zeta_j = \frac{z_j(\cos \psi - p_j(\psi) \sin \psi) + \sqrt{(z_j(\cos \psi - p_j(\psi) \sin \psi))^2 - (a^2 + p_j(\psi)^2 b^2)}}{a - ip_j(\psi)b} \quad (27b)$$

and

$$z_j = x_1 + p_j x_2, \quad p_j(\psi) = \frac{p_j \cos \psi - \sin \psi}{p_j \sin \psi + \cos \psi} \quad (27c)$$

satisfies for particular  $\mathbf{f}$  the condition at infinity (7). Here,  $a$  is the axis of the rotated ellipse lying on the rotated coordinate axis  $\hat{x}_1$  and  $b$  is lying on the rotated coordinate axis  $\hat{x}_2$ . The angle of ellipse

rotation is denoted  $\psi$  as in Fig. 2. The solution in Eq. (27) can be split into several parts

$$\begin{aligned} \frac{1}{\pi} \Im(\mathbf{A} \langle \ln \zeta_* \rangle \mathbf{A}^T) \mathbf{f} &= \frac{1}{\pi} \Im \left( \mathbf{A} \left\langle \ln \frac{z_*}{r_0} \right\rangle \mathbf{A}^T \right) \mathbf{f} + \frac{1}{2\pi} \mathbf{K} \mathbf{f} \\ &\quad - \frac{1}{\pi} \Im \left( \mathbf{A} \left\langle \ln \left( \frac{a - ip_* (\psi) b}{2r_0} \right) \right\rangle \mathbf{A}^T \right) \mathbf{f} - \frac{1}{2\pi} \mathbf{K} \mathbf{f} \\ &\quad + \frac{1}{\pi} \Im \left( \mathbf{A} \left\langle \ln \left( \frac{\frac{z_*}{\cos \psi + p_* \sin \psi} + \sqrt{\left( \frac{z_*}{\cos \psi + p_* \sin \psi} \right)^2 - (a^2 + p_*^2 (\psi) b^2)}}{2z_*} \right) \right\rangle \mathbf{A}^T \right) \mathbf{f}. \end{aligned} \tag{28}$$

It is clear that the first two right-hand side terms form  $\mathbf{U}(x, 0) \mathbf{f}$ . Therefore, the rest of the right-hand side terms must vanish for  $\|x\| \rightarrow +\infty$  and for an appropriate non-zero  $\mathbf{f}$  at a degenerate scale. This implies, calculating the limit in the last term and using the relation (47) from Appendix B, that at a degenerate scale we have

$$\det \left[ \frac{1}{\pi} \Im \left( \mathbf{A} \left\langle \ln \left( \frac{a_c - ip_* (\psi) b_c}{2r_0} \right) \right\rangle \mathbf{A}^T \right) + \frac{1}{2\pi} \mathbf{K} - \mathbf{Z}(\psi) \right] = 0. \tag{29}$$

Having  $a_c = \rho_c a$  and  $b_c = \rho_c b$ , the degenerate scale factor  $\rho_c$  can be found by solving the following eigenvalue problem, because  $-2\Im(\mathbf{A}\mathbf{A}^T) = \mathbf{H}$ :

$$\det \left[ \frac{1}{\pi} \Im \left( \mathbf{A} \left\langle \ln \left( \frac{a - ip_* (\psi) b}{2r_0} \right) \right\rangle \mathbf{A}^T \right) + \frac{1}{2\pi} \mathbf{K} - \mathbf{Z}(\psi) - \frac{1}{2\pi} \ln \rho_c \mathbf{H} \right] = 0. \tag{30}$$

In a special case for  $b \rightarrow 0, \psi = 0$ , and  $\mathbf{K} = \mathbf{0}$ , Eq. (30) reduces to  $\det \left( -\frac{1}{2\pi} \ln \frac{\rho_c a}{2r_0} \mathbf{H} \right) = 0$ . The matrix  $\mathbf{H}$  is positive definite so that for a rigid line inclusion oriented along  $x_1$  axis, there is only one degenerate scale for  $\rho_c = 2 \frac{r_0}{a}$ . In another special case for  $b = a$  ( $\psi = 0$  naturally), a circle, Eq. (30) reduces to  $\det \left( -\frac{1}{2\pi} \left( \ln \frac{\rho_c a}{r_0} \mathbf{H} + \bar{\mathbf{Z}} - \mathbf{K} \right) \right) = 0$ , due to Eq. (47), cf. also Eq. (17). Hence, a circle has generally three different degenerate scales, if the fundamental solution (2) or (42) is used. Nevertheless, for a special choice  $\mathbf{K} = \bar{\mathbf{Z}}$ , Eq. (30) renders only one degenerate scale factor  $\rho_c = \frac{r_0}{a}$  for a circle.

4.1.2. Numerical solution

In the numerical solution, let us consider first an elliptic domain as shown in Fig. 3. The major semi-axis is placed on the  $x_1$  axis as shown and its length is set to unity. The length of the minor semi-axis is varied within the range from (almost) zero to one. In such a way, we can find the degenerate scales for a set of various elliptic domains. The boundary of any ellipse of any material is discretized by a quasi-uniform boundary element mesh which consists of 160 elements.

Three degenerate scale factors of material O are shown in Fig. 4(a). The degenerate scale factors are getting close to 2 where the minor semi-axis is approaching zero, which is in accordance with the analytical solution. The graph shows the points (marked by diamonds) of actually numerically calculated degenerate scale factors and the lines which correspond to the analytical solution of the relation (30) for  $\rho_c$ . The difference between them cannot be distinguished.

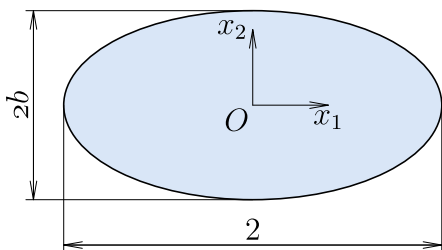


Fig. 3. Dimensions of the reference ellipse.

As we mentioned, the degenerate scales for a circular domain are generally three different when the fundamental solution (2) is used. It is interesting that the variations in material parameters caused the difference between the greatest and other two degenerates scale factors much bigger ( $\rho_{c1} = 1.195712659, \rho_{c2} = 0.501248547, \rho_{c3} = 0.343154045$ ) than in other materials.

Similarly, the other material situations are proceeded. In the case of the material C, the degenerate scale factors are shown in Fig. 4(b). The comparison of the analytical and numerical results confirms again usefulness of the formula (24) as there is no real difference between both ways of evaluation.

The instance of a circle is again pointed out, to see that it provides three degenerate scales and to compare the differences between them ( $\rho_{c1} = 1.343868775, \rho_{c2} = 1.000131598, \rho_{c3} = 0.77264604$ ).

Finally, the material M provides the degenerate scale factors plotted in Fig. 5(a). The results confirm the previous observations.

Nevertheless, the axes of the ellipse and the material axes do not have to coincide. Let us rotate the ellipse by an angle  $\psi = \frac{\pi}{9}$ , cf. Fig. 2, and calculate by SGBEM and the formula (24) the degenerate scale factors. Here, for  $b \rightarrow 0$  the ellipse converts to a line which, however, is not parallel to the  $x_1$  axis. Thus, there is no need of having one triple degenerate scale. The comparison of numerical and analytical results is in Fig. 5(c).

Neither in the case of rotation by an angle  $\psi = \frac{\pi}{2}$  one triple degenerate scale is maintained. The graphs in Fig. 5(d) demonstrate the pertinent values. For the case of a circle  $b = 1$  the degenerate scale factors in Fig. 5(a), (c) and (d) should coincide. The three calculated values are  $\rho_{c1} = 1.261450181, \rho_{c2} = 1.016325174, \rho_{c3} = 0.790678273$ .

Nevertheless, if instead of rotating the ellipse, the axes of material are rotated, the triple degenerate scale remains for the case  $b \rightarrow 0$ . Fig. 5(b) shows the degenerate scale factors in the case, where the material axes have been rotated by an angle  $\phi = \frac{\pi}{2}$  around the axis  $x_3$ . The rotation of the material naturally changes also the fundamental solution, which is still defined by the formula (2), as now the  $x_1$  axis pertains to another material axis. This can be documented e.g. by the degenerate scale factors for a circle ( $a = b$ ) which read  $\rho_{c1} = 1.244978448, \rho_{c2} = 0.984044956, \rho_{c3} = 0.774221089$  and are different from the previous ones.

In all of the instances, the estimate of  $R$  – the radius of surrounded disk, obtained from Eq. (17) which guarantees the positiveness of the operator  $\mathcal{U}_{\Omega}$ , coincides with the smallest degenerate scale of the circle as all the ellipses in the test fit within a circle of a unit radius.

To assess the accuracy of numerical solutions in previous calculations, a convergence test has been performed. In this case, various boundary element meshes have been used: starting with the coarsest mesh which includes only  $N = 10$  elements, subsequently refining the mesh by splitting each element into two, and terminating by a pretty fine mesh of  $N = 320$  elements. The degenerate scale factors calculated for the material case M are summarized in Table 2. All the degenerate scales are calculated for the minor semi-axis  $b = \frac{4}{5}$ . The numerically obtained degenerate scale factors are extrapolated using a three-parameter function  $\rho_c(N) = \hat{\rho}_c + KN^{-\alpha}$ . The extrapolated value  $\hat{\rho}_c$  is compared to that one obtained by the analytical formula (30). It is interesting that the rates of convergence  $\alpha$  are close to two, probably due to smoothness of the elliptic boundary.

4.2. A rectangle

The second numerical simulation is performed for a rectangular domain in Fig. 6. The degenerate scales for the rectangle are again obtained for various ratios of its sides. One side,  $a$ , is set to a constant unit length, the other side  $b$  is changed between (almost) zero and one. In this way, for  $b \rightarrow 0$  we obtain again a line inclusion

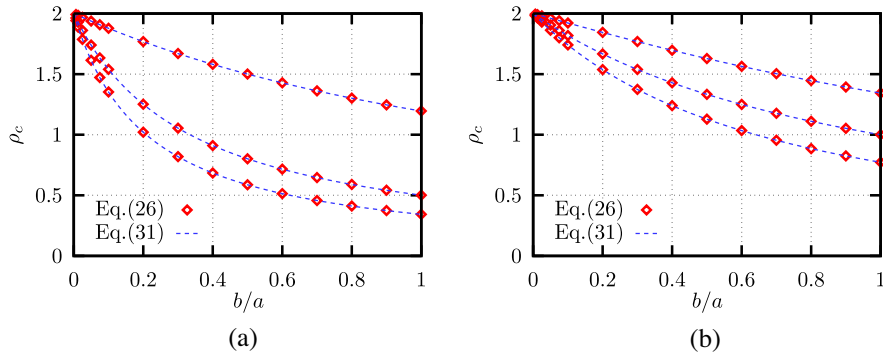


Fig. 4. Degenerate scale factors for elliptic boundary: (a) material O, (b) material C.

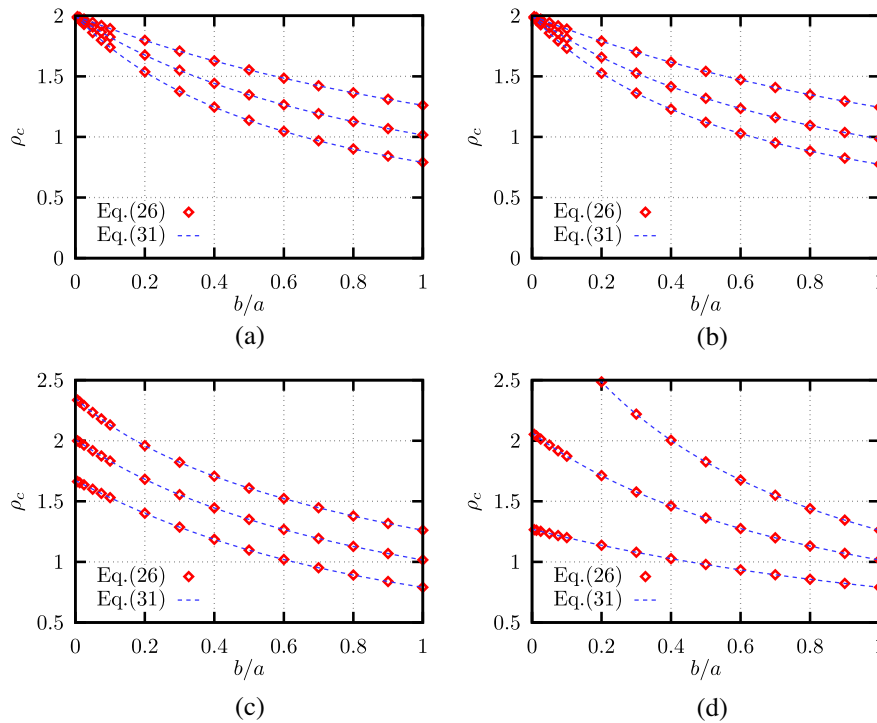


Fig. 5. Degenerate scale factors for elliptic boundary, material M: (a)  $\psi = 0$ , (b)  $\psi = 0$ , rotated material ( $\phi = \frac{\pi}{2}$ ), (c)  $\psi = \frac{\pi}{7}$ , (d)  $\psi = \frac{\pi}{5}$ .

Table 2

Approximations of degenerate scale factors for various discretizations, ellipse with  $b = \frac{4}{5}$ ,  $a = 1$ , material M.

$N$	$\rho_{c1}$	$\rho_{c2}$	$\rho_{c3}$
10	0.9312108344	1.1656224834	1.4144640972
20	0.9083584005	1.1366903219	1.3768078292
40	0.9026924387	1.1294872913	1.3674899708
80	0.9012740593	1.1276808766	1.3651542225
160	0.9009189569	1.1272282603	1.3645687739
320	0.9008302372	1.1271151301	1.3644223858
$\bar{\rho}_c$	0.9008005262	1.1270771838	1.3643732644
$\alpha$	1.9983983702	1.9973184186	1.9968108662
Eq. (30)	0.9008009091	1.1270777181	1.3643739382

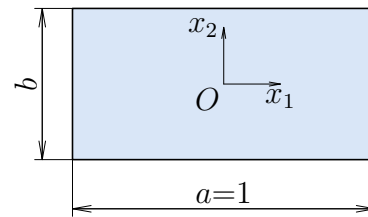


Fig. 6. Dimensions of the reference rectangle.

parallel to the  $x_1$  axis which implies a triple degenerate scale. As long as the length of  $a$  corresponds to  $2a$  in the case of ellipse in Section 4.1, this degenerate scale factor has value of 4.

The boundary element mesh for the numerical solution now contains 160 equally spaced elements along the side  $a$ . The number of elements on  $b$  is adapted in order all the elements to have the same length. For each type of the material the same mesh is used.

The comparison of numerical results obtained by solving the equations in (10) followed by eigenvalue problem (24) is gathered in Figs. 7, and 8(a). Here, no analytical solution is available so that graphs contain smoothed curves connecting the calculated values marked by diamond suit marks. Additionally, each picture includes a dashed line which is an upper bound of guaranteed positive  $U_{\rho r}$  according to the estimate obtained from the relation (17) and a paragraph below. For a rectangle of the dimensions  $1 \times b$ , the smallest circle which covers it has a radius  $r = \frac{1}{2}\sqrt{1+b^2}$ . Similarly to the previous example, the circle radius ensuring the positiveness

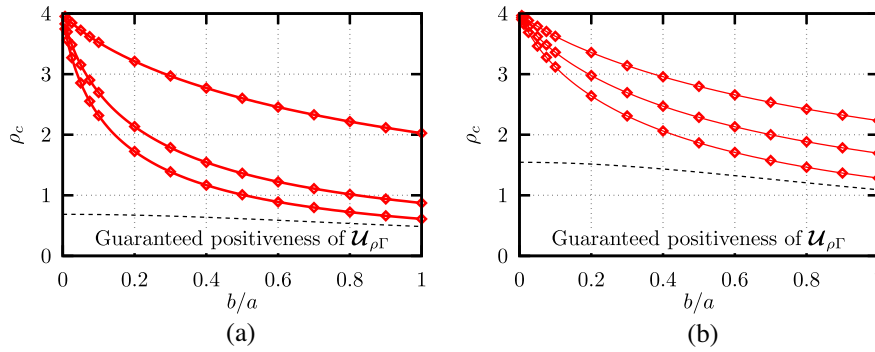


Fig. 7. Degenerate scale factors for the rectangle: (a) material O, (b) material C.

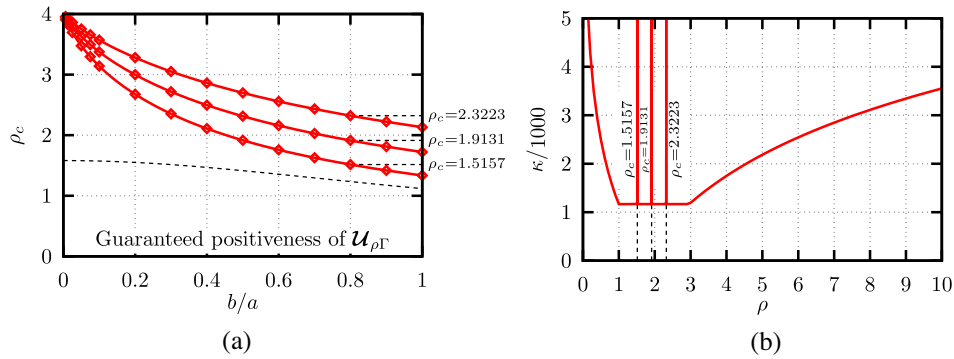


Fig. 8. The rectangular boundary, material M: (a) Degenerate scale factors, (b) Condition number of the  $\mathcal{U}_r$  discretization,  $b = \frac{4}{5}a$ .

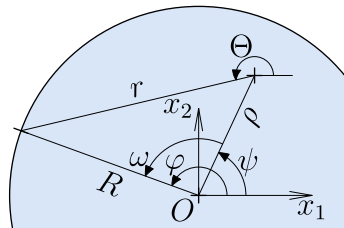


Fig. 9. Geometry parameters defined for a circle.

of  $\mathcal{U}_{\rho\Gamma}$  is  $R = \frac{\rho_{c\min}}{r}$ , where  $\rho_{c\min}$  is the smallest degenerate scale factor for the circle for pertinent material.

Finally, let us try to find the degenerate scales from the properties of the matrix of the operator  $\mathcal{U}_r$  obtained by the aforementioned SGBEM discretization. At a degenerate scale, the integral operator has a nontrivial null-space. Thus, its matrix should be singular or almost singular. As a measure of close-to-singularity, we take the condition number  $\kappa$  defined as the ratio between the greatest and the smallest singular value, (Golub and van Loan, 1983), which gives infinity for a singular matrix. To this end, a series of rectangles with an aspect ratio 4 : 5 has been taken together with the material M and a boundary element mesh of 40 elements per a rectangle side. The reference rectangle is that of Fig. 6. Fig. 8(b) shows the condition number  $\kappa$  of the SGBEM discretization matrix depending on the scaling factor  $\rho$ . It is clear that near to a degenerate scale,  $\kappa$  increases without bounds. Three peaks correspond to the three degenerate scales of the reference rectangle. Besides, it can be seen that both for  $\rho \rightarrow 0$  and  $\rho \rightarrow +\infty$  the condition number of the matrix behaves logarithmically and that the peaks appear somewhere in a plateau part of the graph. Nevertheless, it is difficult to find the peaks numerically as they are very narrow. A very fine stepping of  $\rho$  should be used to find them. In the graphs, the width of any of the three peaks is less than 0.01 near the plateau level. Anyhow, the

peaks coincide with the values of the degenerate scale factors which can be seen in both pictures of Fig. 8.

5. Conclusion

The problem of determination of degenerate scales associated to the boundary  $\Gamma$  of the domain  $\Omega$ , for which the (generalized plane strain) anisotropic elastic single-layer potential operator  $\mathcal{U}_r$  is not invertible, has been studied. A formula for degenerate scale factors was derived based on reformulation of the problem with a matrix of the operator  $B_\Gamma$  whose generalized eigenvalues in relation with the Barnett–Lothe tensor  $\mathbf{H}$  determine the degenerate scales. In such a way, there are three degenerate scales for a general anisotropic material as it has been shown. If considering standard plane strain isotropic elasticity two degenerate scales are obtained. It is caused by the fact that the antiplane deformations, in the present case  $u_3$ , are uncoupled from the inplane deformations in such a particular case and they are discussed separately. The solution of pertinent DBVP for antiplane deformations then provides the additional degenerate scale. However, the inplane and antiplane deformations cannot be uncoupled for a general anisotropic material.

Although, the numerical tests were performed with simple boundary shapes, the derived formula for determining the degenerate scales can be applied to any shape and size of the domain and its boundary.

The integral kernel of the operator  $\mathcal{U}_r$  defined by the fundamental solution of the Navier equation was introduced with two options: a scalar  $r_0$  and a constant symmetric matrix  $\mathbf{K}$ , in order to have tools either to guarantee the positiveness of the operator  $\mathcal{U}_r$  for a particular domain or to set specified degenerate scale factors to required values, e.g. to ones for a circle. Both modifications can be useful in practical calculations.

Although not discussed all in the present paper, the results of the author's previous works (Vodička and Mantič, 2004b;

Vodička, 2013) may be, after some modification, implemented for anisotropic materials, namely: independence of the degenerate scales on the number and position of holes for an interior domain and asymptotic behavior of the degenerate scales for an exterior BVP with multiple holes.

**Acknowledgments**

The authors acknowledge the financial support from the Scientific Grant Agency of the Slovak Republic VEGA (Grant No. 1/0201/11). The author R.V. would also like to thank Prof. Vladislav Mantič, University of Seville, who motivated him to think anisotropically.

**Appendix A. Calculation of the integral on a circle**

Let us calculate the integral  $\int_{\Gamma_R} \mathbf{U}(x, y) d\Gamma(y)$  for  $\Gamma_R$  being a circle of radius  $R$  and for a point  $x$  lying in the interior of the circle.

The matrix  $\mathbf{U}$  in Eq. (2) can be split into three parts. The first one depends on  $r$  only. Based on Fig. 9, we can write

$$y_1 = R \cos \varphi, \quad x_1 = \rho \cos \psi, \quad r^2 = R^2 + \rho^2 - 2R\rho \cos(\varphi - \psi),$$

$$y_2 = R \sin \varphi, \quad x_2 = \rho \sin \psi, \quad \Theta = \arctan\left(\frac{R \sin \varphi - \rho \sin \psi}{R \cos \varphi - \rho \cos \psi}\right). \quad (31)$$

The pertinent integral to calculate is

$$\int_{\Gamma_R} \ln r d\Gamma = \frac{R}{2} \int_{-\pi+\psi}^{\pi+\psi} \ln(R^2 + \rho^2 - 2R\rho \cos(\varphi - \psi)) d\varphi$$

$$= \frac{R}{2} \int_{-\pi}^{\pi} \ln(R^2 + \rho^2 - 2R\rho \cos \omega) d\omega. \quad (32)$$

It does not depend on  $\psi$  and as we intend to show it neither depends on  $\rho$ , therefore it does not depend on the choice of  $x$ . Actually, let us differentiate the integral (32) with respect to  $\rho$  ( $R > \rho > 0$ ) to obtain

$$\frac{R}{2} \int_{-\pi}^{\pi} \frac{2\rho - 2R \cos \omega}{R^2 + \rho^2 - 2R\rho \cos \omega} d\omega \stackrel{\tan \frac{\omega}{2} = t}{=} 2R \int_{-\infty}^{+\infty} \frac{(R+\rho)t^2 - (R-\rho)}{(R+\rho)^2 t^2 + (R-\rho)^2 t^2 + 1} \frac{1}{t^2 + 1} dt$$

$$= \frac{R}{\rho} \left[ \arctan t - \arctan \frac{R+\rho}{R-\rho} t \right]_{-\infty}^{+\infty} = 0, \quad (33)$$

which proves that the integral is constant with respect to  $\rho$ . Making a limit for  $\rho \rightarrow 0^+$  or for  $\rho \rightarrow R^-$  does not change the value of integral in (33), as e.g.

$$\lim_{\rho \rightarrow 0^+} \frac{R}{\rho} \left[ \arctan t - \arctan \frac{R+\rho}{R-\rho} t \right]_{-\infty}^{+\infty} = \frac{1}{R} \left[ \frac{-2t}{t^2 + 1} \right]_{-\infty}^{+\infty} = 0. \quad (34)$$

Hence, the integral can be calculated for  $\rho = 0$  and the same value is valid for all interior points of the circle. The calculation renders

$$\int_{\Gamma_R} \ln r d\Gamma = \frac{R}{2} \int_{-\pi}^{\pi} \ln(R^2) d\omega = 2\pi R \ln R. \quad (35)$$

For the second integral (the function  $\mathbf{Z}(\Theta)$ ) we use rather following parameterization

$$y_1 - x_1 = r(\Theta) \cos \Theta, \quad r(\Theta) = -\rho \cos(\Theta - \psi) + \varrho(\Theta - \psi),$$

$$y_2 - x_2 = r(\Theta) \sin \Theta, \quad d\Gamma = \frac{Rr(\Theta)}{\varrho(\Theta - \psi)} d\Theta, \quad (36)$$

with  $\varrho(\theta) = \sqrt{R^2 - \rho^2 \sin^2(\theta)}$ . The integral reads

$$\int_{\Gamma_R} \mathbf{Z}(\Theta) d\Gamma = R \int_{-\pi}^{\pi} \mathbf{Z}(\Theta) \frac{-\rho \cos(\Theta - \psi) + \varrho(\Theta - \psi)}{\varrho(\Theta - \psi)} d\Theta. \quad (37)$$

As above, we again show that it depends neither on  $\psi$  nor on  $\rho$ , therefore it does not depend on the choice of  $x$ . Actually, let us differentiate the integral (37) with respect to  $\rho$  to obtain

$$R^3 \int_{-\pi}^{\pi} \mathbf{Z}(\Theta) \frac{\cos(\Theta - \psi)}{\varrho^3(\Theta - \psi)} d\Theta = R^3 \int_0^{\pi} \mathbf{Z}(\Theta) \frac{\cos(\Theta - \psi)}{\varrho^3(\Theta - \psi)} d\Theta$$

$$+ R^3 \int_0^{\pi} \mathbf{Z}(\Theta - \pi) \frac{\cos(\Theta - \pi - \psi)}{\varrho^3(\Theta - \pi - \psi)} d\Theta$$

$$= R^3 \int_0^{\pi} \mathbf{Z}(\Theta) \frac{\cos(\Theta - \psi)}{\varrho^3(\Theta - \psi)} d\Theta$$

$$+ R^3 \int_0^{\pi} \mathbf{Z}(\Theta) \frac{-\cos(\Theta - \psi)}{\varrho^3(\Theta - \psi)} d\Theta = 0 \quad (38)$$

due to periodicity of  $\mathbf{Z}(\Theta)$ , Eq. (48). Similarly, the differentiation of the integral (37) with respect to  $\psi$  renders

$$R\rho(R^2 - \rho^2) \int_{-\pi}^{\pi} \mathbf{Z}(\Theta) \frac{\sin(\Theta - \psi)}{\varrho^3(\Theta - \psi)} d\Theta = 0 \quad (39)$$

and the reasoning is the same as for Eq. (38). Hence, the integral is constant and can be calculated for  $\rho = 0$ . The calculation renders

$$\int_{\Gamma_R} \mathbf{Z}(\Theta) d\Gamma = R \int_{-\pi}^{\pi} \mathbf{Z}(\Theta) d\Theta = R\bar{\mathbf{Z}}. \quad (40)$$

To conclude by adding the integral of a constant matrix  $\mathbf{K}$ , we have for any  $x$  in the interior of  $\Gamma_R$

$$\int_{\Gamma_R} \mathbf{U}(x, y) d\Gamma(y) = \int_{\Gamma_R} -\frac{1}{2\pi} \ln \frac{r}{r_0} \mathbf{H} - \mathbf{Z}(\Theta) + \frac{1}{2\pi} \mathbf{K} d\Gamma$$

$$= -R \left( \ln \frac{R}{r_0} \mathbf{H} + \bar{\mathbf{Z}} - \mathbf{K} \right). \quad (41)$$

**Appendix B. Algebraic representation of  $\mathbf{U}$  based on the Stroh formalism**

The fundamental solution (2) can be alternatively expressed in a purely algebraic form using the sextic formalism of Stroh, see e.g. Ting (1996). It then reads as

$$\mathbf{U}(x, y) = \frac{1}{\pi} \Im \left( \mathbf{A} \operatorname{diag} \left( \ln \frac{z_1}{r_0}, \ln \frac{z_2}{r_0}, \ln \frac{z_3}{r_0} \right) \mathbf{A}^{\top} \right) + \frac{1}{2\pi} \mathbf{K}, \quad (42)$$

with  $z_i = (y_1 - x_1) + p_i(y_2 - x_2) = r(\cos \Theta + p_i \sin \Theta)$ ,  $i = 1, 2, 3$ ,  $\Im(z)$  denoting the imaginary part of a complex number  $z$  and the principal branch of the complex logarithmic function  $\ln z = \ln |z| + i \operatorname{Arg}(z)$ . We can also formalize  $\operatorname{diag}(\ln z_1, \ln z_2, \ln z_3)$  as  $\langle \ln \mathbf{z} \rangle$ .

The material parameters in  $\mathbf{A}$  (also in  $\mathbf{B}$  below) and  $p_i$  are expressed in the terms of eigenvalues and eigenvectors of the matrix  $\mathbf{N} = \begin{pmatrix} -\mathbf{T}^{-1} \mathbf{R}^{\top} & \mathbf{T}^{-1} \\ -\mathbf{Q} + \mathbf{R} \mathbf{T}^{-1} \mathbf{R}^{\top} & -\mathbf{R} \mathbf{T}^{-1} \end{pmatrix} = \begin{pmatrix} \mathbf{N}_1 & \mathbf{N}_2 \\ \mathbf{N}_2^{\top} & \mathbf{N}_3 \end{pmatrix}$ , cf. (4) and (3a). Namely, using the structure of the matrix  $\mathbf{N}$ , they can be obtained as

$$\begin{pmatrix} \mathbf{N}_1 & \mathbf{N}_2 \\ \mathbf{N}_2^{\top} & \mathbf{N}_3 \end{pmatrix} \begin{pmatrix} \mathbf{A} & \bar{\mathbf{A}} \\ \mathbf{B} & \bar{\mathbf{B}} \end{pmatrix} = \begin{pmatrix} \mathbf{A} & \bar{\mathbf{A}} \\ \mathbf{B} & \bar{\mathbf{B}} \end{pmatrix} \begin{pmatrix} \mathbf{P} & \mathbf{0} \\ \mathbf{0} & \bar{\mathbf{P}} \end{pmatrix}, \quad (43)$$

where  $\mathbf{P} = \operatorname{diag}(p_1, p_2, p_3)$ , all  $p_i$  are imaginary in any case and  $\Im(p_i) > 0$ . It should be noted that the form of Eq. (43) requires the matrix  $\mathbf{N}$  to have six linearly independent eigenvectors even in the case where some of the eigenvalues  $p_i$  are the same. If this is not the case, the material is called degenerate and the matrix diagonalization as in Eq. (43) has a bit different form, see Ting (1996). The matrices  $\mathbf{A}$  and  $\mathbf{B}$  can be chosen to satisfy the relation

$$\begin{pmatrix} \mathbf{A} & \bar{\mathbf{A}} \\ \mathbf{B} & \bar{\mathbf{B}} \end{pmatrix} \begin{pmatrix} \mathbf{B}^{\top} & \mathbf{A}^{\top} \\ \bar{\mathbf{B}}^{\top} & \bar{\mathbf{A}}^{\top} \end{pmatrix} = \begin{pmatrix} \mathbf{I} & \mathbf{0} \\ \mathbf{0} & \mathbf{I} \end{pmatrix} = \begin{pmatrix} \mathbf{B}^{\top} & \mathbf{A}^{\top} \\ \bar{\mathbf{B}}^{\top} & \bar{\mathbf{A}}^{\top} \end{pmatrix} \begin{pmatrix} \mathbf{A} & \bar{\mathbf{A}} \\ \mathbf{B} & \bar{\mathbf{B}} \end{pmatrix}. \quad (44)$$

Using this notation, the Barnett–Lothe tensors in Eq. (3) read as

$$\mathbf{S}(\Theta) = \frac{2}{\pi} \Re(\mathbf{A}(\ln(\cos \Theta + p_* \sin \Theta))\mathbf{B}^\top), \quad (45a)$$

$$\mathbf{H}(\Theta) = \frac{2}{\pi} \Re(\mathbf{A}(\ln(\cos \Theta + p_* \sin \Theta))\mathbf{A}^\top), \quad (45b)$$

$$-\mathbf{L}(\Theta) = \frac{2}{\pi} \Re(\mathbf{B}(\ln(\cos \Theta + p_* \sin \Theta))\mathbf{B}^\top), \quad (45c)$$

where  $\Re(z)$  denotes the real part of a complex number  $z$ .

The relations (45), together with Eq. (3b) provide useful shifting formulae for the Barnett–Lothe tensors

$$\begin{aligned} \mathbf{S}(\Theta + \pi) &= \mathbf{S}(\Theta) + \mathbf{S}, \quad \mathbf{H}(\Theta + \pi) = \mathbf{H}(\Theta) + \mathbf{H}, \quad \mathbf{L}(\Theta + \pi) \\ &= \mathbf{L}(\Theta) + \mathbf{L}. \end{aligned} \quad (46)$$

These relations could also be seen as consequences of the integral representation (3a), realizing the periodicity of the matrix functions  $\mathbf{Q}(\Theta)$ ,  $\mathbf{R}(\Theta)$  and  $\mathbf{T}(\Theta)$  in Eq. (4a).

Substituting Eq. (45) into  $\mathbf{Z}(\Theta)$  introduced in Eq. (2) and calculating  $\bar{\mathbf{Z}}$  (cf. Eq. (15)) by integration, we obtain

$$\begin{aligned} \mathbf{Z}(\Theta) &= -\frac{1}{\pi} \Im(\mathbf{A}(\ln(\cos \Theta + p_* \sin \Theta))\mathbf{A}^\top), \\ \bar{\mathbf{Z}} &= -2\Im\left(\mathbf{A}\left\langle \ln \left[ \frac{1}{2}(1 - ip_*) \right] \right\rangle \mathbf{A}^\top\right). \end{aligned} \quad (47)$$

The matrix function  $\mathbf{Z}(\Theta)$  is periodic with a period  $\pi$  as follows from the relation

$$\begin{aligned} \mathbf{Z}(\Theta + \pi) &= \frac{1}{2}(\mathbf{H}\mathbf{S}^\top(\Theta + \pi) + \mathbf{S}\mathbf{H}(\Theta + \pi)) \\ &= \frac{1}{2}(\mathbf{H}(\mathbf{S}^\top(\Theta) + \mathbf{S}^\top) + \mathbf{S}(\mathbf{H}(\Theta) + \mathbf{H})) = \mathbf{Z}(\Theta), \end{aligned} \quad (48)$$

because of the known identity  $\mathbf{H}\mathbf{S}^\top + \mathbf{S}\mathbf{H} = \mathbf{0}$ . Equivalently, it can be seen from Eq. (47)<sub>1</sub> as  $\Re(\mathbf{A}\mathbf{A}^\top) = \mathbf{0}$  due to Eq. (44).

The integral to be calculated in Eq. (47)<sub>2</sub> is  $\mathbf{J}(p) = \int_{-\pi}^{+\pi} \ln(\cos \Theta + p \sin \Theta) d\Theta$  for a complex number  $p$ . It is clear that

$$\begin{aligned} \frac{d\mathbf{J}(p)}{dp} &= \int_{-\pi}^{+\pi} \frac{\sin \Theta}{\cos \Theta + p \sin \Theta} d\Theta \stackrel{t=\tan \frac{\Theta}{2}}{=} \int_{-\infty}^{+\infty} \frac{-4t}{(1+t^2)(t^2-2pt-1)} dt \\ &= \int_{-\infty}^{+\infty} \mathbf{f}(t) dt = 2\pi i \sum_{b_j \in B} \text{Res}_{z=b_j} \mathbf{f}(z) = 2\pi i (\text{Res}_{z=i} \mathbf{f}(z) \\ &\quad + \text{Res}_{z=p+\sqrt{1+p^2}} \mathbf{f}(z) + \text{Res}_{z=p-\sqrt{1+p^2}} \mathbf{f}(z)) = \frac{2\pi}{i+p} \end{aligned} \quad (49)$$

using the residue theorem for  $B$  being a set of poles of the function  $\mathbf{f}$  with positive imaginary parts (Evgrafov, 1976). Here,  $\text{Res}_{z=z_0} \mathbf{f}(z)$  denotes the complex residue of function  $\mathbf{f}(z)$ , i.e. the coefficient  $a_{-1}$  in the Laurent series  $\mathbf{f}(z) = \sum_{k=-\infty}^{+\infty} a_k(z-z_0)^k$  of the function  $\mathbf{f}$  about the point  $z_0$ . The number  $\tilde{p} = \sqrt{1+p^2}$  is the complex square root of the number  $1+p^2$  with the positive imaginary part. It can be shown that for  $\Im(p) > 0$  both  $p \pm \tilde{p}$  have positive imaginary parts. Of course, there is an exception of  $p = i$  for which all three poles coincide and  $i$  is a triple pole of the function  $\mathbf{f}$  from (49). In this particular case,  $\text{Res}_{z=i} \mathbf{f}(z) = -\frac{1}{2}$  so that the result of Eq. (49) fortunately still holds. The residues to produce the result of Eq. (49) in the all other situations are

$$\text{Res}_{z=i} \mathbf{f}(z) = \frac{1-ip}{1+p^2}, \quad \text{Res}_{z=p \pm \sqrt{1+p^2}} \mathbf{f}(z) = \frac{-1}{1+p^2}. \quad (50)$$

Hence, with the aid of  $\int_{-\pi}^{+\pi} \ln(\cos \Theta + i \sin \Theta) d\Theta = 0$  we can write

$$\begin{aligned} \mathbf{J}(p) &= \int_{-\pi}^{+\pi} \ln(\cos \Theta + p \sin \Theta) d\Theta = 2\pi \ln(i+p) + C \\ 0 = \mathbf{J}(i) &= 2\pi \ln(i+i) + C = 2\pi(\ln 2 + i\frac{\pi}{2}) + C \end{aligned} \Rightarrow \mathbf{J}(p) = 2\pi \ln \frac{1}{2}(1-ip) \quad (51)$$

and the relation between the left and right equation in Eq. (47) is now obvious.

References

Blázquez, A., Mantić, V., París, F., 2006. Application of BEM to generalized plane problems for anisotropic elastic materials in presence of contact. *Eng. Anal. Bound. Elem.* 30 (6), 489–502.

Bonnet, M., Maier, G., Polizzotto, C., 1998. Symmetric Galerkin boundary element method. *Appl. Mech. Rev.* 15, 669–704.

Chen, Y.Z., 2011. Numerical solution for degenerate scale problem arising from multiple rigid lines in plane elasticity. *Appl. Math. Comput.* 218, 96–106.

Chen, Y.Z., Lin, X.Y., 2008. Regularity condition and numerical examination for degenerate scale problem of BIE for exterior problem of plane elasticity. *Eng. Anal. Bound. Elem.* 32, 811–823.

Chen, J.T., Kuo, S.R., Lin, J.H., 2002a. Analytical study and numerical experiments for degenerate scale problems in the boundary element method for two-dimensional elasticity. *Int. J. Numer. Methods Eng.* 54, 1669–1681.

Chen, J.T., Lee, C.F., Chen, I.L., Lin, J.H., 2002b. An alternative method for degenerate scale problems in boundary element method for the two-dimensional Laplace equation. *Eng. Anal. Bound. Elem.* 26, 559–569.

Chen, J.T., Lin, S.R., Chen, K.H., 2005. Degenerate scale problem when solving Laplace's equation by BEM and its treatment. *Int. J. Numer. Methods Eng.* 62, 233–261.

Chen, Y.Z., Lin, X.Y., Wang, Z.X., 2009a. Evaluation of the degenerate scale for BIE inplane elasticity and antiplane elasticity by using conformal mapping. *Eng. Anal. Bound. Elem.* 33, 147–158.

Chen, Y.Z., Lin, X.Y., Wang, Z.X., 2009b. Numerical solution for degenerate scale problem for exterior multiply connected region. *Eng. Anal. Bound. Elem.* 33, 1316–1321.

Chen, Y.Z., Wang, Z.X., Lin, X.Y., 2009c. The degenerate scale problem for the Laplace equation and plane elasticity in a multiply connected region with an outer circular boundary. *Int. J. Solids Struct.* 46, 2605–2610.

Chen, Y.Z., Wang, Z.X., Lin, X.Y., 2009d. A new kernel in BIE and the exterior boundary value problem in plane elasticity. *Acta Mech.* 206, 207–224.

Chen, J.T., Han, H., Kuo, S.R., Kao, S.K., 2014. Regularization methods for ill-conditioned system of the integral equation of the first kind with the logarithmic kernel. *Inverse Probl. Sci. Eng.* 22 (7), 1176–1193.

Chou, T.H., 1970. *Elastic Constants of Monoclinic Potassium Cobaltcyanide* (McGill theses, Thesis, M. Eng.). McGill University.

Christiansen, S., 1982. On two methods for elimination of non-unique solutions of an integral equation with logarithmic kernel. *Appl. Anal.* 13, 1–18.

Christiansen, S., 1985. Modifications of some first kind integral equations with logarithmic kernel to improve numerical conditioning. *Computing* 34, 221–242.

Christiansen, S., 1998. Derivation and analytical investigation of three direct boundary integral equations for the fundamental biharmonic problem. *J. Comput. Appl. Math.* 91, 231–247.

Christiansen, S., 2001. Detecting non-uniqueness of solutions to biharmonic integral equations through SVD. *J. Comput. Appl. Math.* 134, 23–35.

Constanda, C., 1994. On non-unique solutions of weakly singular integral equations in plane elasticity. *Quart. J. Mech. Appl. Math.* 47, 261–268.

Constanda, C., 1995. Integral equations of the first kind in plane elasticity. *Quart. Appl. Math.* 53 (4), 783–793.

Corfdir, A., Bonnet, G., 2013. Degenerate scale for the Laplace problem in the half plane; approximate logarithmic capacity for two distant boundaries. *Eng. Anal. Bound. Elem.* 37 (5), 836–841.

Corfdir, A., Bonnet, G., 2014. Variational formulation and upper bounds for degenerate scales in plane elasticity. *J. Elasticity*. <http://dx.doi.org/10.1007/s10659-014-9494-1>.

Costabel, M., 1988. Boundary integral operators on Lipschitz domains: elementary results. *SIAM J. Math. Anal.* 19 (3), 613–626.

Costabel, M., Dauge, M., 1996. Invertibility of the biharmonic single layer potential operator. *Integr. Equ. Oper. Theory* 24, 46–67.

Dijkstra, W., Mattheij, R.M.M., 2008. Condition number of the BEM matrix arising from the Stokes equations in 2D. *Eng. Anal. Bound. Elem.* 32 (9), 736–746.

Evgrafov, M.A., 1976. *Analytic Functions*. Saunders.

Golub, G.H., van Loan, C.F., 1983. *Matrix Computations*. The Johns Hopkins University Press, Baltimore, Maryland.

Gurtin, M., 1972. The linear theory of elasticity. In: Flügge, S. (Ed.), *Encyclopedia of Physics*. Springer Verlag, Berlin, pp. 1–295.

He, W.J., Ding, H.J., Hu, H.C., 1996. A necessary and sufficient boundary integral formulation for plane elasticity problems. *Commun. Numer. Methods Eng.* 12, 413–424.

Heise, U., 1978. The spectra of some integral operators for plane elastostatical boundary value problems. *J. Elasticity* 8 (1), 47–79.

Heise, U., 1987. Dependence of the round-off error in the solution of boundary integral equations on geometrical scale factor. *Comput. Methods Appl. Mech. Eng.* 62, 115–126.

Hsiao, G.C., 1986. On the stability of integral equations of the first kind with logarithmic kernels. *Arch. Ration. Mech. Anal.* 94, 179–192.

Hsiao, G.C., Wendland, W.L., 1985. On a boundary integral method for some exterior problems in elasticity. In: *Proc. Tbil. Univ., UDK 539.3, Math. Mech. Astron.*, pp. 31–60.

Hwu, C., 2010. *Anisotropic Elastic Plates*. Springer, New York.

- Ivančo, V., Vodička, R., 2012. Numerické metódy mechaniky telies a vybrané aplikácie. Technická univerzita v Košiciach, Košice (in Slovak).
- Jaswon, M.A., Symm, G.T., 1977. *Integral Equation Methods in Potential Theory and Elastostatics*. Academic Press, London, London.
- Kress, R., Spassov, W.T., 1983. On the condition number of boundary integral operators for the exterior Dirichlet problem for the Helmholtz equation. *Numer. Math.* 42, 77–85.
- Kuhn, G., Löbel, G., Potřč, I., 1987. Kritisches Lösungsverhalten der direkten Randelementmethode bei logarithmischen Kern. *ZAMM* 67, 361–363.
- Kuo, S.R., Chen, J.T., Lee, J.W., Chen, Y.W., 2013. Analytical derivation and numerical experiments of degenerate scales for regular N-gon domains in two-dimensional Laplace problems. *Appl. Math. Comput.* 219, 5668–5683.
- Mantič, V., París, F., 1998. Integral kernels in the 2D Somigliana displacement and stress identities for anisotropic materials. *Comput. Mech.* 22 (1), 77–87.
- McLean, W., 2000. *Strongly Elliptic Systems and Boundary Integral Equations*. Cambridge University Press, Cambridge.
- Požgaj, A., Chovanec, D., Kurjatko, S., Babiak, M., 1977. Štruktúra a vlastnosti dreva. *Príroda* (in Slovak).
- Shiah, Y.C., Tan, C.L., 2000. Determination of interior point stresses in two dimensional BEM thermoelastic analysis of anisotropic bodies. *Int. J. Solids Struct.* 37 (5), 809–829.
- Simmons, G., Wang, H., 1971. *Single Crystal Elastic Constants and Calculated Aggregate Properties: A handbook*. MIT Press.
- Steinbach, O., Wendland, W.L., 2001. On C. Neumann's method for second-order elliptic systems in domains with non-smooth boundaries. *J. Math. Anal. Appl.* 262, 733–748.
- Ting, T.C.T., 1996. *Anisotropic Elasticity. Theory and Applications*. Oxford University Press, Oxford.
- Vodička, R., 2013. An asymptotic property of degenerate scales for multiple holes in plane elasticity. *Appl. Math. Comput.* 220, 166–175.
- Vodička, R., Mantič, V., 2004a. On invertibility of boundary integral equation systems in linear elasticity. *Build. Res. J.* 52, 1–18.
- Vodička, R., Mantič, V., 2004b. On invertibility of elastic single layer potential operator. *J. Elasticity* 74, 147–173.
- Vodička, R., Mantič, V., 2008. On solvability of a first-kind boundary integral equation for Dirichlet boundary value problems in plane elasticity. *Comput. Mech.* 41 (6), 817–826.
- Yan, Y., Sloan, I.H., 1988. Integral equations of the first kind with logarithmic kernels. *J. Integ. Equ. Appl.* 1 (4), 549–579.